Deep-Sea Research II 91 (2013) 139–151

Contents lists available at SciVerse ScienceDirect

Deep-Sea Research II

journal homepage: www.elsevier.com/locate/dsr2

A comparison of North Pacific and North Atlantic subtropical mode waters in a climatologically-forced model

Elizabeth M. Douglass *, Young-Oh Kwon, Steven R. Jayne

Woods Hole Oceanographic Institution, Woods Hole, Massachusetts, USA

ARTICLE INFO

Available online 27 February 2013

Keywords:
Mode water
Interannual variability
Subtropical gyre
Ventilation

ABSTRACT

Subtropical mode water (STMW), a water mass with homogeneous temperature and density and low potential vorticity, is formed in the subtropical gyres of both the North Pacific and North Atlantic Oceans. In the North Atlantic, this water mass is known as Eighteen Degree Water (EDW), while the corresponding water mass in the Pacific is identified as North Pacific Subtropical Mode Water (NPSTMW). This analysis compares properties of EDW with NPSTMW as well as the intrinsic oceanic variability of both, within the framework of a high resolution model with climatological atmospheric forcing. Interannual variability is evident in both volume and characteristics of EDW and NPSTMW, but the magnitude of variability is small, indicating that observed variability is largely forced by atmospheric changes. Volume of EDW is greater than volume of NPSTMW, but volume variability is similar in the two basins, and is dominated by the seasonal cycle in both cases. The most significant differences are found in the average ages of EDW compared to NPSTMW. Although the volume of STMW formed in each basin is similar, different circulation patterns lead to a higher average age in the North Atlantic, as EDW is more likely to be advected away from the formation region and remain subducted in the North Atlantic, while NPSTMW is more likely to be reventilated the following winter in the North Pacific.

1. Introduction

The subtropical Atlantic and Pacific Oceans have many similarities. In each, the most significant feature is the western boundary current. In the Atlantic, the Gulf Stream follows the coast of North America, and separates at Cape Hatteras, near 35°N. In the Pacific, the Kuroshio follows the coast of Japan and turns eastward in the Kuroshio Extension, at the Bōsō Peninsula, also near 35°N. After separation, both of these western boundary currents head eastward with jet-like structures, and both have southern subtropical recirculation gyres. In the winter, strong winds create a deep mixed layer, with the deepest regions just south of the jets. When restratification occurs in the spring, this deep mixed layer with uniform temperature and low potential vorticity is capped by the seasonal thermocline, preserving its homogeneity. This thermostad is the subtropical mode water (STMW).

In the Atlantic, this well-known water mass is called Eighteen Degree Water (EDW), and is easily identified by its consistent temperature (Worthington, 1959). Observations indicate that this water mass has temperature around 18 °C, density near 26.5 kg m^{-3}, and low potential vorticity (Joyce et al., 2009; Talley and Raymer, 1982). In the Pacific, a similarly formed thermostad is named North Pacific Subtropical Mode Water (NPSTMW) (Masuzawa, 1969). Its temperature characteristics are not as consistent and are slightly cooler, with the temperature varying from 16° to 18 °C. Density is also lower, between 25.0 and 25.5 kg m^{-3}, consistent with lower salinity in the Pacific Ocean (Hanawa and Suga, 1995; Suga et al., 2008). The low potential vorticity, however, is comparable (Hanawa and Talley, 2001). In both oceans, STMW represents a unified water mass, whose characteristics are important indicators of the ventilation of the upper ocean, the circulation and its structure, and the interaction with the atmosphere.

Variability of the volume of STMW has been documented through observations in both the Atlantic and the Pacific (Joyce et al., 2000; Oka, 2009; Suga and Hanawa, 1995; Suga et al., 1989; Talley and Raymer, 1982). In the Atlantic, there is a clear correlation between volume of EDW and the North Atlantic Oscillation (Joyce et al., 2000; Kwon and Riser, 2004). In the Pacific Ocean, it has been hypothesized that volume of NPSTMW is modulated by changes in monsoonal forcing (Suga and Hanawa, 1995; Qiu and Chen, 2006) or by changes in the Kuroshio Extension (Qiu and Chen, 2006; Qiu et al., 2006). However, these changes in the Kuroshio Extension are thought to be forced

* Correspondence to: Woods Hole Oceanographic Institution, MS #29, 266 Woods Hole Road, Woods Hole, MA 02543, USA
E-mail address: edouglass@whoi.edu (E.M. Douglass).

0967-0645/$ - see front matter © 2013 Elsevier Ltd. All rights reserved.
http://dx.doi.org/10.1016/j.dsr2.2013.02.023

by changes in large-scale wind stress curl associated with the Pacific Decadal Oscillation (Qiu and Chen, 2005). As a result, in both basins, atmospheric variations dominate variability in ocean circulation. This analysis will elucidate differences in intrinsic oceanic variability in the basins. Differences between the North Atlantic and North Pacific basins include the characteristics of the Kuroshio and the Gulf Stream, the width of the basins, and the formation of deep water in the North Atlantic that is not found in the North Pacific. By suppressing atmospheric variability, the ocean model run used in this analysis will help define differences in the variability of STMW due to sources other than the large-scale atmospheric changes. The model is forced with climatological atmospheric forcing, allowing analysis of the intrinsic variability of the nonlinear ocean system, rather than the variability arising from large scale changes in the atmospheric component of the coupled ocean–atmosphere system.

The goal of this paper is to compare and contrast the characteristics and variability of STMW in the North Pacific and North Atlantic oceans. The comparison is simplified by the fact that a single eddy-resolving integration is used to provide output for both regions. Comparisons with observations in each region are used to indicate how well model performs in some respects, but the main focus here is on comparisons between the variability and characteristics in the two separate basins.

2. Model description

The model used here is the Parallel Ocean Program (POP), an ocean general circulation model that solves the 3-dimensional primitive equations for ocean dynamics (Smith and Gent, 2002; Smith et al., 2010). The output is the same as that used in Maltrud et al. (2010), including the use of a tripole grid, which alleviates having a singularity in the ocean at the North Pole. This grid has two singularities in the northern hemisphere, both located over land (North America and Asia), to eliminate singularities within the ocean (Murray, 1996). The model was run globally for 120 years with annually repeating surface atmospheric conditions, downward radiative fluxes and precipitation, prescribed from a climatology blending National Center of Environmental Prediction–National Center for Atmospheric Research (NCEP–NCAR) reanalysis products and remote sensing products, known as normal-year forcing (Large and Yeager, 2009). Air–sea heat and moisture fluxes are computed using the prescribed atmospheric state and the model predicted sea surface temperature (SST) through standard bulk formulae. Intrinsic oceanic variability leads to SST variations, which change the calculated heat and moisture fluxes on non-seasonal timescales, but this variation is small in comparison to the seasonal cycle. The model has 42 vertical levels, ranging from 10 m near the surface to 250 m at depth. The top 500 m is comprised of 19 levels, so the depths at which STMW exist are relatively well-resolved. Horizontal spacing is approximately 0.1° in both latitude and longitude, allowing resolution of mesoscale features such as eddies. Monthly averaged fields of temperature, salinity, sea surface height (SSH), and zonal, meridional, and vertical velocity are stored as output. Several additional diagnostic fields such as ideal age and potential vorticity are also stored. Years 0 through 19 were considered spinup, and output was available for years 20 through 119 for temperature, salinity, SSH, ideal age, and all velocity fields. The model was run globally, but this analysis is limited to the North Pacific and North Atlantic. Snapshots of SSH in the study region are shown in Fig. 1, along with SSH from altimetry for comparison. The basic structure of the model is the same as the observations, and the magnitude and scale of mesoscale variability is similar in the model and the data. In both basins, the western boundary currents separate from the coast at approximately the right latitude. The main difference between observations and model output is that the observed SSH gradient across the jet is not as strong as that in the model. The models have higher SSH in the recirculation gyre to the south of the jet, and lower SSH north of the jet, indicating a stronger current. These differences are more evident in looking at the mean SSH, but the snapshots of SSH are shown to demonstrate the realistic representation of mesoscale variability in the model.

3. Identifying STMW

The first step in this analysis is to identify the criteria used to determine whether a given water parcel is considered to be STMW. The generally warmer and saltier nature of the Atlantic Ocean is reflected in the different temperature and density ranges used to define NPSTMW and EDW. Both water masses are also required to be within a range of potential vorticity, defined here as

$$Q \equiv -\frac{f}{\rho}\frac{\partial \sigma_\theta}{\partial z} \tag{1}$$

In either basin, potential vorticity is a measure of stratification, and low stratification is indicative of the homogeneous nature of STMW.

Observationally, and in the present analysis, NPSTMW is defined as having temperature between 16 and 20 °C, density between 25.0 and 25.5 kg m^{-3}, and potential vorticity below 2×10^{-10} m^{-1}s^{-1} (Hanawa and Suga, 1995; Masuzawa, 1969; Rainville et al., 2007). Additionally, the thickness of the layer must be greater than 50 m. This restriction excludes transient shallow surface layers that appear seasonally. These layers are within the temperature range of NPSTMW, but are not persistent or significant. These restrictions are in accord with previous research, and their applicability here demonstrates that NPSTMW is well represented in this model.

In the Atlantic, on the other hand, analysis shows that there is a warm bias in model output relative to historical data. As mentioned previously, STMW in the North Atlantic is commonly known as Eighteen Degree Water, and one would expect the vast majority of the water to indeed be approximately 18 °C (Talley and Raymer, 1982; Worthington, 1959). However, the thick layer with homogeneous temperature in the model is slightly warmer than 18 °C. Therefore, for this analysis, EDW is defined as having temperature between 17 and 21 °C. The density range suggested in the literature (26.2–26.6 kg m^{-3}) (Talley, 1996) must be modified to fit the conditions as well, so 25.7–26.2 kg m^{-3} is used instead. The potential vorticity of less than 2×10^{-10} m^{-1}s^{-1} is consistent with the value used in the Pacific Ocean. This is twice the value used by Talley and Raymer (1982) in their analysis of EDW, but given the resolution of the model, the threshold of 1×10^{-10} m^{-1}s^{-1} is too restrictive and would eliminate too much water that should be classifed as EDW. Again, the restriction that thickness must be greater than 50 m excludes transient surface layers.

To illustrate the selection criteria, Fig. 2 shows four cross sections from each ocean. Each of these is a model snapshot from a particular month. Fig. 2A and B show cross sections from the month of March, when the mixed layer is deepest at the end of winter and the STMW is being ventilated. Fig. 2C and D show cross sections from June, after restratification has sequestered the STMW from the surface. Cross sections are from south to north, along the black lines indicated in Fig. 1. In both cases, colors show a thick layer of homogeneous temperature. Thick black contours indicate the potential density range just identified, while thin black contours indicate the temperature range. Gray contours show the potential vorticity of 2×10^{-10} m^{-1}s^{-1}. The white cross-hatched region is the STMW. The figure clearly shows the outcropped STMW in March in both oceans, and the thick layer

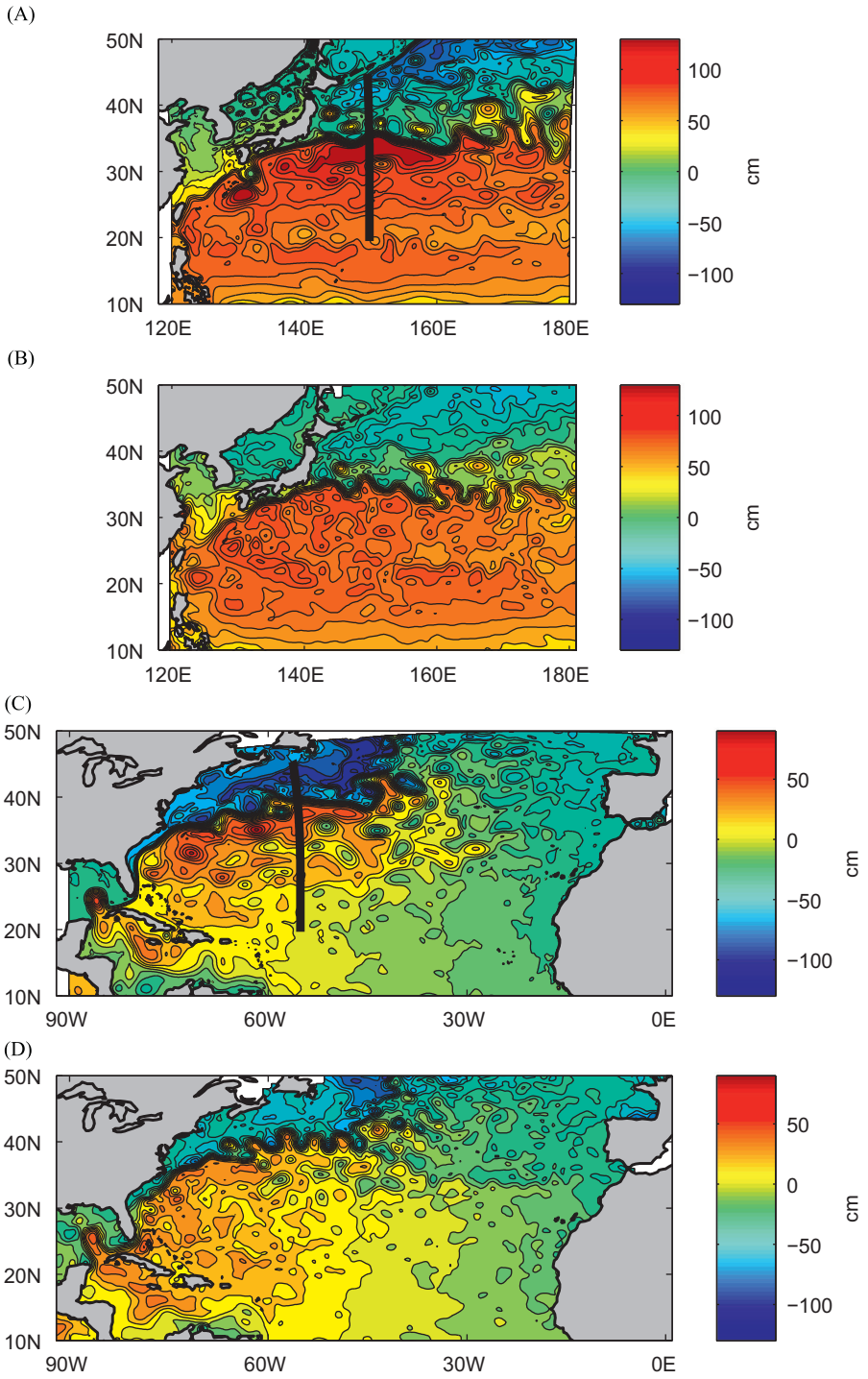

Fig. 1. (A) Snapshot of SSH in North Pacific subtropical gyre from model output in March of year 50. (B) Snapshot of SSH from Aviso altimetry data in March 1993. (C) and (D) are as (A) and (B), but for the Atlantic instead of the Pacific. Contour interval is 10 cm in each figure. Thick black lines in (A) and (C) indicate locations of sections used for description of STMW in Fig. 2.

beneath the summertime stratification in June. Year 50 of the model run is used for this illustration.

4. Formation

The process of STMW formation is similar in the two oceans. In this analysis, formation is defined as ventilation of water with the properties of STMW. Thus, a column of water with the temperature, density, potential vorticity and layer thickness associated with STMW, in contact with the surface, is considered newly formed STMW. Using this definition, maps of formation locations are shown in Fig. 3A and B for the Pacific and the Atlantic, respectively. Contours indicate the average annual STMW formation during the 100 year model run, and a thick magenta line shows the average location of the Kuroshio in the Pacific and the Gulf Stream in the Atlantic. In each basin, formation occurs south and east of the western boundary currents. In the Pacific, the maximum STMW formation occurs just south of the semipermanent meander after the Kuroshio

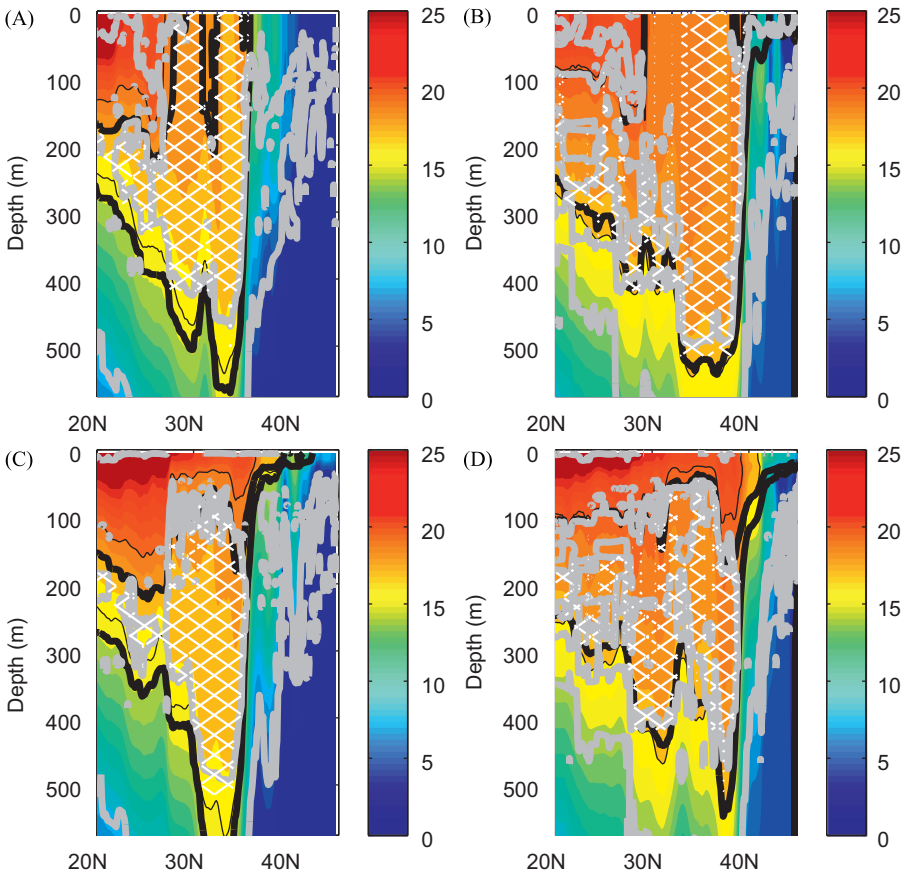

Fig. 2. Example of STMW in late winter, while it is being ventilated (March) and summer, after restratification has sequestered it (June), in both oceans, in model year 50. Colors show temperature, thin black contours are temperature above and below the STMW, thick black contours are density above and below the STMW, and gray contours are PV$=2\times10^{-10}$ m^{-1} s^{-1}. Cross hatched area is the STMW. (For interpretation of the references to color in this figure legend, the reader is referred to the web version of this article.)

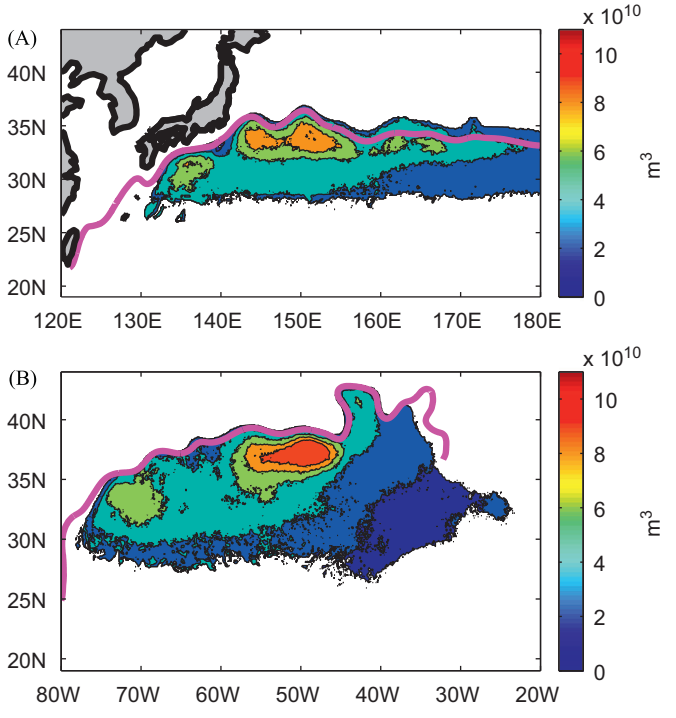

Fig. 3. (A) Location of NPSTMW formation in North Pacific. (B) Location of EDW formation in the Atlantic. The value contoured is the average annual volume of STMW formed at the given location. Thick magenta lines indicate the average contour of the western boundary current. (For interpretation of the references to color in this figure legend, the reader is referred to the web version of this article.)

separates from Japan, near 34°N, 145–150°E. This is consistent with observations (Oka, 2009; Qiu and Chen, 2006). This region has the deepest average wintertime mixed layer in the North Pacific, shown in Fig. 4A. At its northern edge, it is also near the region of strongest wintertime cooling in the North Pacific (Fig. 4B). Note that both the magnitude of the wintertime mixed layer depth and the location of the strongest heat fluxes are in line with those shown in Kelly et al. (2010); the same is true in the Atlantic. The proximity of the maximum formation region to the Kuroshio Extension indicates formation via cross-frontal exchange as described by Worthington (1972). Two other regions of relatively high formation exist, one to the east just south of the Kuroshio Extension, and one to the west in the region south of Japan.

In the Atlantic, the region of maximum formation is farther to the east. Again, maximum formation occurs where deep mixed layers and proximity to the front of the western boundary current and its associated strong heat loss coincide (Fig. 4C and D). Formation in this location, due to cross-frontal processes, was observed by Joyce (2011) in the Atlantic. A second high-formation region occurs further west, in the center of the Sargasso Sea in the southern recirculation gyre, centered at approximately 70°W, 33°N. This is analogous to the region just south of Japan. Formation of EDW in the center of the Sargasso Sea has been described by Warren (1972). The two regions of high formation in the Atlantic agree with the description suggested by Joyce (2011) based on observations from the CLIMODE experiment. More generally, similar maps of formation have been presented by Maze et al. (2009). While the exact extent of the formation region varies some between different estimates and methodologies, the

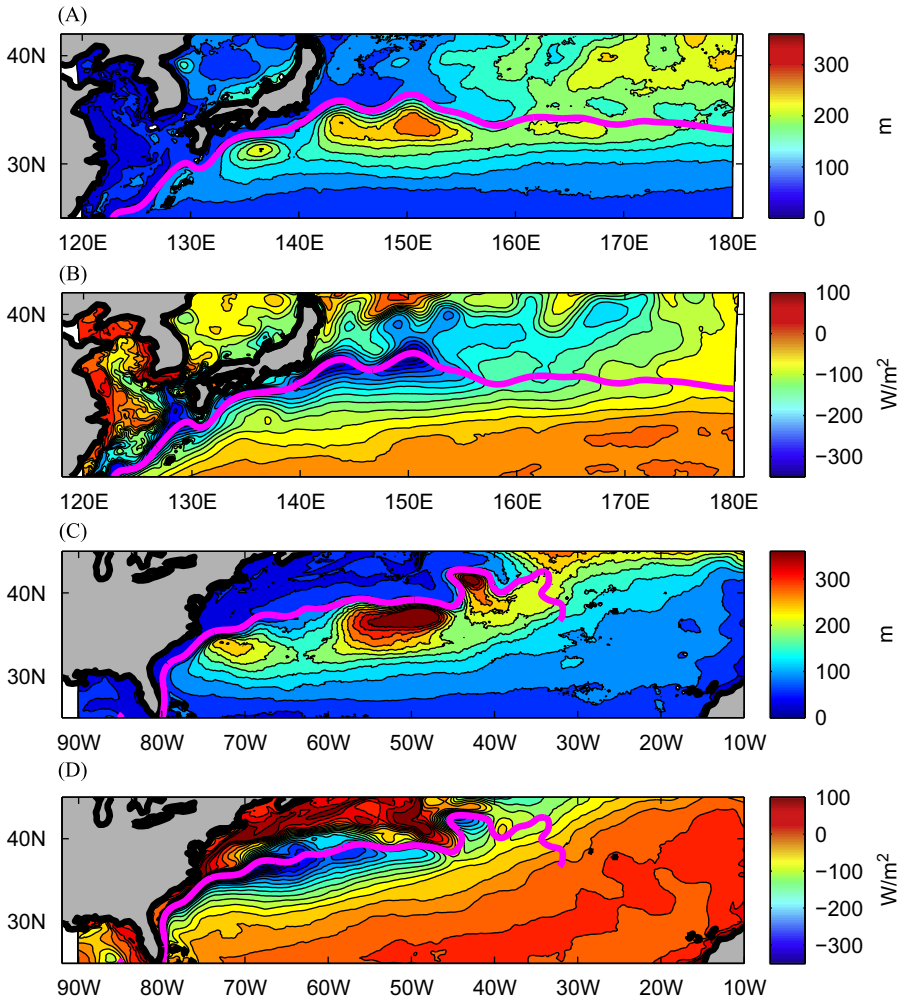

Fig. 4. (A) Wintertime (JFM) mixed layer depth in North Pacific. (B) Winter (JFM) heat flux in the North Pacific. (C) Wintertime mixed layer depth in the Atlantic. (D) Winter (JFM) heat flux in the Atlantic. Thick magenta lines indicate the average contour of the western boundary current. (For interpretation of the references to color in this figure legend, the reader is referred to the web version of this article.)

general structure of EDW formation is consistent. Thus, the two basins show formation in analogous locations: in the recirculation gyre, and south of the front of the western boundary current. In both basins, formation only occurs north of 28°N, as was also noted by Oka (2009). Maximum formation occurs farther east in the Atlantic, but in both basins STMW is formed primarily where the deepest mixed layers occur in the winter, and secondarily in the recirculation gyres associated with the western boundary currents. In both basins, variability in total mode water is closely related to variability in formation. In the Atlantic, the correlation between the annually averaged formation (as shown in Fig. 5B) and the annual averaged total volume of mode water is 0.77. In the Pacific, the correlation is 0.69. This indicates that changes in formation are responsible for most of the changes in total mode water volume, and to understand this variability, we should understand what causes changes in formation.

There are several possible sources for the variability in formation. A detailed discussion of this issue as it relates to the Pacific can be found in Douglass et al. (2012). Their conclusion is that outcrop area is the governing factor in the Pacific, and that other possibly important factors like local eddy kinetic energy are relatively unchanging. Accordingly we proceed by discussing the changes in outcrop area in the two basins.

The time series of outcrop area in each region is shown in Fig. 5. A smoothed time series is created by taking the average of March and April of each year, since these are the months of maximum STMW formation. In both basins, there is some variability but no long term trends or patterns. Variability in outcrop area is reflected in the volume of STMW formed. In the Atlantic, the correlation between surface outcrop area and volume of STMW formation is 0.79, and in the Pacific, it is 0.93, indicating the importance of variability in outcrop area on the variability in formation. The lower correlation in the Atlantic is largely due to a long-term trend. It should be noted that while this trend is evident in several aspects of the analysis in the Atlantic, there are no spatial patterns associated with it. When the detrended time series are compared, the correlation is 0.88. This trend is only found in the Atlantic, and is evident in the change in volume and will be demonstrated in other characteristics of EDW later in this analysis. In both basins, the volume of newly ventilated STMW increases slightly in time, but the percentage of total STMW being ventilated remains approximately constant.

There are several things that could cause changes in outcrop area. One of the most obvious would be changes in heat flux, but given the annually repeating imposed atmospheric forcing in this model output, any changes in the heat flux would be due to the changes in the ocean. These would most likely result from changes in the strong western boundary currents. Three aspects of the western boundary currents are analyzed in each basin. First, the latitude of the western boundary current could change.

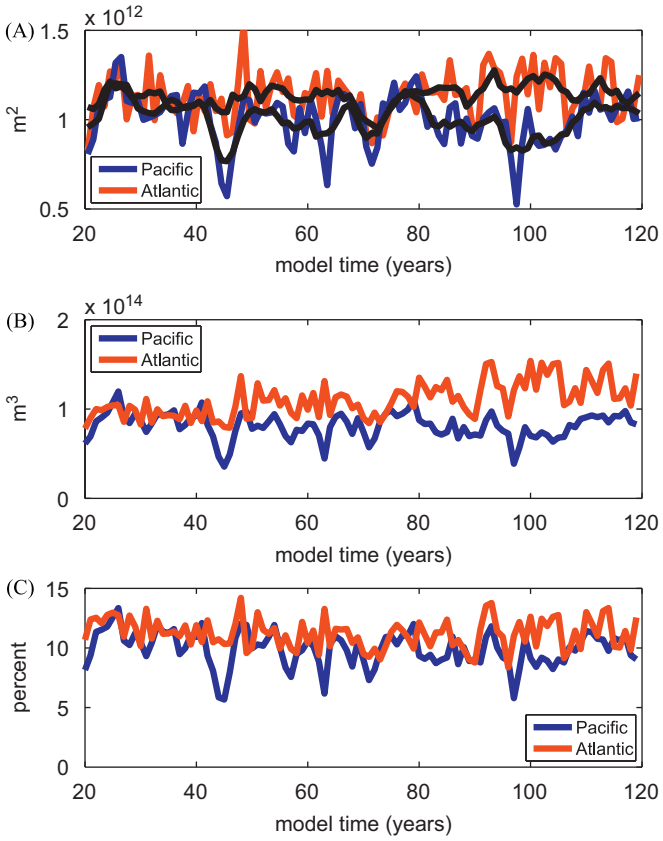

Fig. 5. (A) Surface area of outcropping where STMW is formed, in each basin, as shown in Fig. 3. Black lines show 5-year smoothing. (B) Time series of newly ventilated STMW in each basin. (C) Newly ventilated STMW normalized by total STMW volume, to show percentage of STMW being ventilated.

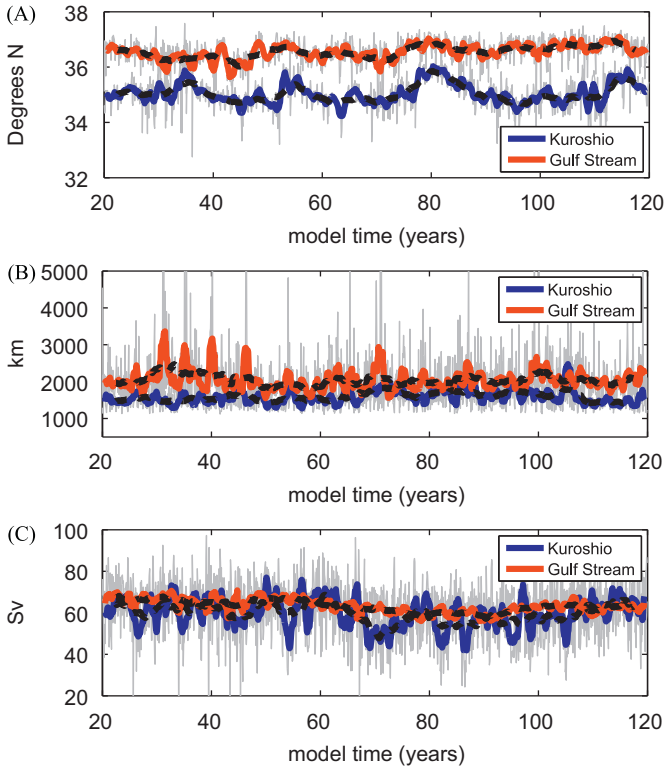

Fig. 6. (A) Latitude of Kuroshio and Gulf Stream after separation. (B) Path length of Kuroshio and Gulf Stream after separation. (C) Transport of the Kuroshio and Gulf Stream near the separation point. In all panels, thin gray lines show full time series, thick colored lines show smoothing over one year, and thick black dashed lines show 5-yr smoothing. (For interpretation of the references to color in this figure legend, the reader is referred to the web version of this article.)

A more northerly Kuroshio or Gulf Stream could lead to greater air–sea temperature difference in a larger area, thus a larger outcrop area, and therefore, more formation of mode water. Alternatively, the meandering of the current must be examined. The Kuroshio in particular has been found to have strongly and weakly meandering states. As a proxy for this, the path length of the western boundary current after separation from the coast is examined. A higher path length should indicate a more strongly meandering current. Finally, the variability of transport of the WBC is analyzed. As a simple way of finding the transport, the depth-averaged velocity of the current, at the axis of the current, from the surface to 1500 m is multiplied by depth and an average current width of 100 km. This rough calculation shows the variability of the depth-averaged current in the top 1500 m, translated into units of Sverdrups (1 Sverdrup=1 Sv=10^6 m^3 s^{-1}). The average latitude after separation, the path length after separation, and the transport for each current are shown in Fig. 6.

Variability is evident in each of these quantities. Correlations between the latitude of the western boundary currents and the associated outcrop areas are relatively low (r=0.37 in each basin), when the time series have been smoothed over one year. When smoothing over 5 years is applied, more significant correlations emerge, with correlation coefficients of 0.49 in the Pacific and 0.63 in the Atlantic. Thus, the interannual to decadal variability evident in the meridional location of the Kuroshio or the Gulf Stream influences the outcrop area where STMW is formed.

Although the month-to-month variability of the path length appears high, when smoothed over one year to compare with the yearly changes in outcrop area, no statistically significant correlations exist. On interannual time scales, the path length of the Kuroshio hardly changes at all. While there are changes in the path length of the Gulf Stream, they are not correlated with mode water variability. It is interesting to note that significant interannual changes in path length are observed in the Kuroshio, but these are attributed to variability arising from Rossby waves (Qiu and Chen, 2005). The fact that such variability is not evident in the present simulation confirms that its source is atmospheric rather than oceanic.

The transport is shown in Fig. 6C. Again, short term variability is intense. In the Atlantic, once the time series is smoothed over 12 months it is nearly constant. It is the Kuroshio in this case that retains some variabliity when smoothed over 12 months. Although this variability is present, it is not correlated with outcrop area or volume of mode water formation in either basin.

5. Ideal age

Ideal age is a model variable indicating the length of elapsed time since a given water parcel has been in contact with the surface. When a given water parcel is in contact with the surface, its ideal age is set to zero, and when the parcel is not in contact with the surface, ideal age increments with time. Thus, it is an estimate of the ventilation time scale. The average ideal age of the STMW in each basin is shown in Fig. 7A. Since ideal age is initialized to zero everywhere at the beginning of the model run, equilibration must be accounted for. For deeper water masses with longer time scales, equilibration can take hundreds or even thousands of years, but it is expected that since STMW is relatively shallow and is ventilated with some regularity, it will equilibrate more quickly. Still, the trend in age of STMW seen in

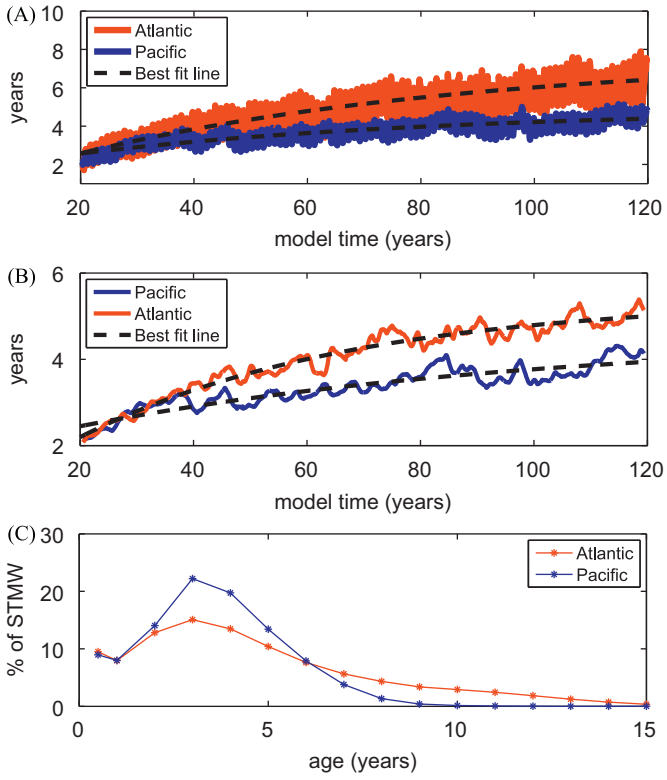

Fig. 7. (A) Time series of average ideal age of STMW in each basin, with best fit line. (B) Time series of core age of STMW in each basin, with best fit line. (C) Distribution of ideal ages of STMW in each basin.

Fig. 7 is not unexpected. Even in the presence of such a trend, comparisons between the two regions, which are subsets of the same model run and therefore have the same shortcomings regarding reaching equilibrium, are still valid. We can conclude from the faster increase in the age of EDW that EDW lives longer without being reventilated or destroyed. Averaged over the time series, the age of EDW is 4.94 years, while that of NPSTMW is 3.70 years. However, in both basins, the age will eventually equilibrate. To estimate the age at equilibrium, a curve of the form

$$\text{age} = a(1-e^{-t/\lambda})+c \quad (2)$$

was fit to the time series of age in each basin. In this equation, t is time and c is age at the start of the time series. Age will eventually asymptote to $a+c$, and λ is a time decay constant. Fig. 7A shows the average age in each basin, along with the best fit lines as established by this method. The age of EDW will asymptote to 7.6 years, while the age of NPSTMW approaches 4.9 years.

The core age can be defined as the age at the depth of the core, where the "core" of mode water is the depth of minimum PV. The other core properties will be discussed later in the manuscript. The trend seen in average age is also evident in core age (Fig. 7B). As with average age, core age increases faster and is consistently higher in the Atlantic basin. This is indicative of older water retaining the properties of STMW rather than being eroded away. The lower age in the NPSTMW is indicative of a shorter residence time for STMW in the Pacific than in the Atlantic. Using the same fitting scheme, the core age asymptotes to 5.4 years in the Atlantic and 4.6 years in the Pacific. It is expected that core age will be lower than average age, given that the full average will always include some very old STMW, but these should be excluded from the core. From these calculations, the result that EDW is older than NPSTMW is confirmed as robust.

A distribution of the average ages of STMW is seen in Fig. 7C. The distributions of ages in the two basins have very different shapes. These distributions are normalized by total volume of STMW, and as such, indicate the percentage of STMW in each age bin. Both distributions peak around three years. However, the Atlantic distribution also has a much longer tail, indicating small percentages of much older EDW. This is particularly evident in the age bins over 10 years, where the values in the Pacific distribution are indistinguishable from zero, while those in the Atlantic are still 1% or 2%. Averaged over the model run, 6.9% of EDW has ideal age higher than 10 years, compared to 0.1% of NPSTMW. The age distribution at the last time step demonstrates ages when the model is closest to equilibration. In the final year of the model run, 0.9% of the NPSTMW has an ideal age over 10 years, compared to 17.9% of EDW.

There are several ways to estimate the overturning time of the STMW. One method considers annual production and erosion. Kwon and Riser (2004) use the average amount of STMW in early spring (February to April) minus that in winter (November to January) to estimate STMW production. By that metric, the model produces 2.86×10^{14} m^3 of EDW in the Atlantic Ocean, somewhat larger than their estimate of $1.10 \pm 0.16 \times 10^{14}$ m^3. They also divide total STMW by production in each year to determine an overturning time of 3.57 ± 0.54 years. Using the same metric, the model estimates overturning in the Atlantic at 4.56 years. In the Pacific, the model produces an average of 2.31×10^{14} m^3 of STMW, for an overturning time of 3.88 years. This method assumes that new STMW is the only water ventilated in a given year, and that previously formed older water retains its old age. However, it is possible for previously formed STMW to be reventilated; this would not result in a change in STMW volume, but it would reduce the overturning time of the water mass. Since this mechanism is not considered, the estimates from this method can be considered an upper bound on overturning.

On the other hand, the definition of formation of STMW in the present analysis identifies all newly ventilated STMW as newly formed STMW. Thus, previously formed STMW that outcrops in the winter is considered to be newly ventilated STMW with its age set to zero. It is likely that the deepest part of the thermostad is not fully ventilated, and that some STMW would still be old rather than new, so an estimate that assumes full ventilation can be considered a lower bound. This estimate is obtained by dividing the average total volume of STMW by the average volume of STMW ventilated during the peak production late winter months of March and April. The lower bounds for overturning age obtained in this way are 2.52 years in the Atlantic Ocean and 2.46 years in the Pacific Ocean.

In both the Pacific and the Atlantic, newly ventilated STMW comprises approximately 12% of total STMW volume. The differences in average ages must come from differences in the circulation pathways in the two basins. It appears that in the Atlantic, EDW is more likely to remain sequestered from the surface once it is formed. It retains the properties of EDW, and its age increases, as it is not ventilated again. In the Pacific, a layer of NPSTMW is more likely to be reventilated in the winter and have its age reset to zero, reducing the average age of the water mass. Thus in the Atlantic, Fig. 7C shows a long tail in the distribution of older EDW that has retained its properties but has not been in contact with the surface, while in the Pacific the oldest NPSTMW erodes but new NPSTMW forms to take its place. The volume of STMW being ventilated is similar, but in the Atlantic the ventilation reduces the inventory of 3-year-old water while in the Pacific the 3-year-old water accumulates as older water erodes. While other factors such as differences in transport and dissipation will have an effect as well, it is clear that this disparity in ventilation in the two basins leads directly to higher average ages and longer overturning times in the Atlantic.

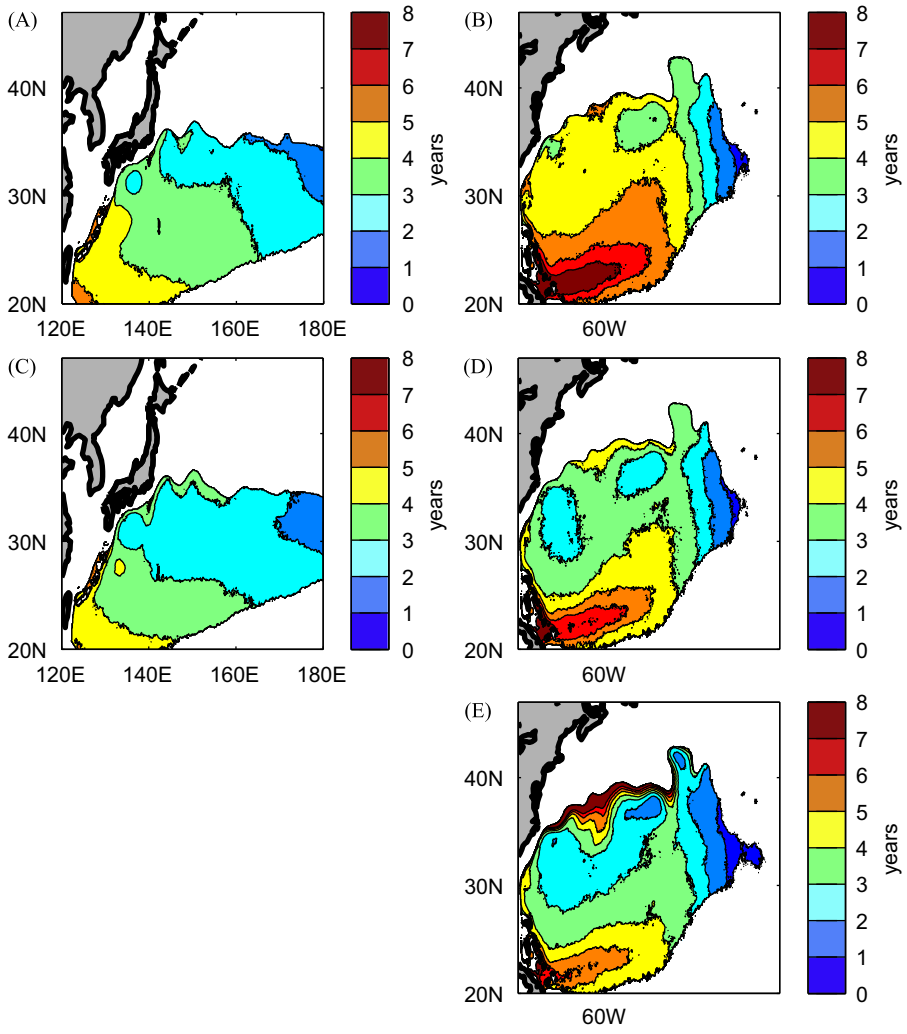

Fig. 8. (A) Average ideal age of STMW in the Pacific. (B) Core ideal age of STMW in the Pacific.(C) and (D) are the same as (A) and (B), but for the Atlantic. Only locations where STMW exists more than 25% of the time are shown. (E) Average core age from TTD in the Atlantic.

A map of ideal age can give a visual indication of where STMW is being ventilated, and where it travels after ventilation. If STMW outcrops every year in a particular location, the average age in that location will be close to zero, while if STMW is advected to a location while subducted, the average age should indicate the time to reach that location. Fig. 8A and C shows such ideal age maps for both basins. Fig. 8B and D shows the maps of core age, which are overall very similar to the average age maps. In many respects, similarities exist between the two basins. STMW is younger in the eastern and northern locations, which were identified in the previous section as locations of formation. In both basins, STMW reaches the oldest ages in the southwest corner of the subtropical gyre. Maps of formation locations show no formation in these areas, so STMW existing in these locations has been advected from elsewhere, without contact with the surface, aging as it traveled. In general, travel pathways follow the streamlines one would expect of large-scale gyre circulation. The maps of age in the Atlantic Ocean have a more complex structure than that in the Pacific. In particular, there is an interesting lobe of very old EDW around 22°N, just east of the Caribbean in the Atlantic, while no similar feature exists in the Pacific. The fact that this lobe is so far south could indicate that EDW in this location is not being mixed away as observations would suggest. Maps of STMW thickness (Fig. 11) show no particular feature in this region; in both basins, STMW is relatively thin at less than 100 m at that latitude. EDW also reaches greater ages, with maximum values near 8, while the NPSTMW seems to have maximum values around 5.

Since ideal age takes time to equilibrate, another method can be used to calculate the average age of the STMW. The model output includes transit time distributions, or TTDs. A transit time distribution simulates the input of a tracer at the surface of the model. This field is set to one every month for a year at the surface, after which it is switched off, by setting it to zero. The field then propagates through the model through advection and diffusion as a passive tracer. The first moment of the time series of the TTD in a water mass is, by definition, the average age of the water mass (Maltrud et al., 2010). In Maltrud et al. (2010), this value is shown not to equilibrate for at least 70 or 80 years at the depths of interest here. There only exists one TTD of that length in the model output, and it was only calculated in the Atlantic. A map of the core age calculated using this method is shown in Fig. 8e. This demonstrates that even using a different method, the same spatial patterns with very similar magnitudes are calculated for the age of the core of the STMW.

6. STMW characteristics

Having discussed the differences between formation in the two basins, and the resulting differences in age of the water mass,

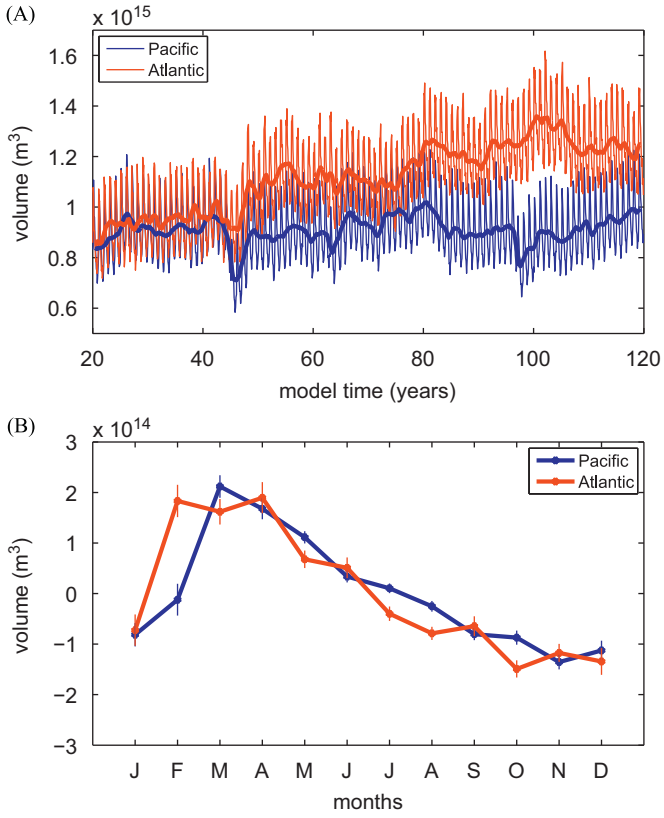

Fig. 9. (A) Time series of volume of STMW in each basin. Thin lines show full time series, thick lines are smoothed with a running mean over 12 months. (B) Mean seasonal cycle of STMW in each basin. Error bars are one standard deviation.

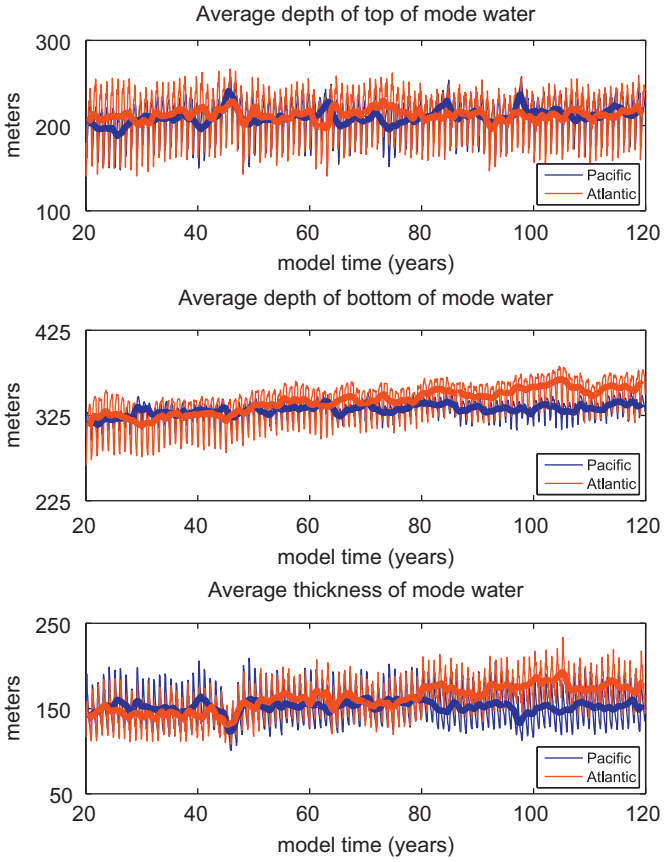

Fig. 10. (A) Time series of average depth of top of STMW layer in each basin. Thin lines show full time series, thick lines are smoothed with a running mean over 12 months. (B) Time series of average depth of bottom of STMW layer in each basin. (C) Time series of average thickness of STMW layer in each basin.

it is also interesting to look at the characteristics of the two mode water masses. This section will compare the total volume of mode water, the thickness of the mode water masses, and the properties at the core of the STMW in each basin.

6.1. Volume

In each basin, a time series can be constructed of the total volume of STMW (Fig. 9A). Thin lines show the full time series, while thick lines have the seasonal cycle removed with a 12-month running mean. For both basins, the volumes are of the order of 1×10^{15} m^3, which is slightly larger than recent estimates. For example, Kwon and Riser (2004) show volumes of EDW around 3.5×10^{14} m^3, and Rainville et al. (2007) use a model to look at NPSTMW and also find 3.5×10^{14} m^3. This could be related to differences in the definition of mode water, or to a broader spatial range in the present analysis than in the other studies. In the present analysis as in other studies, the volume of EDW is very similar to that of NPSTMW initially, but EDW increases throughout the model simulation. This is due to a gradual increase in the thickness of the thermostad, rather than an expansion in spatial area. The thickening results from a deepening of the bottom of the EDW layer, as shown in Fig. 10. This long-term trend is an indication that the model is not fully spun up in the Atlantic. Although this trend will be evident in several aspects of this analysis, most of the analysis will focus on variability after removing the trends, so the conclusions are still relevant. The average volume of NPSTMW is relatively constant. This is reflected throughout the time series in the depth of the tops and bottoms of the STMW, as well as the thickness. If the trend is removed from the EDW, the amplitude of interannual variability is similar in the two oceans. The standard deviation of the smoothed time series of volume of STMW, after removing a linear trend, is 4.9×10^{13} m^3 in the Atlantic Ocean and 5.2×10^{13} m^3 in the Pacific. Thus changes are only on the order of 5% of the mean volume. Spectral analysis indicates that there is no obvious time scale associated with the variability (not shown). The Pacific has two anomalously negative spikes, around years 45 and 98, each of which lasts approximately 3 years, as well as less abrupt variability on the 5–10 year time scale. In the Atlantic, small changes on time scales of 5 years or less are common, while peaks in years 80 and 100 indicate a possibility of multi-decadal variability superimposed on the long-term trend. All of these signals are significantly smaller than the seasonal cycle. It is evident that the large variability in interannual STMW volume disappears when atmospheric variability is removed.

The seasonal cycles in both ocean basins are the most significant, persistent signal in STMW volume, with magnitude far exceeding any interannual variability. This is different from observations in the Atlantic, where interannual variability associated with the North Atlantic Oscillation has been shown to affect EDW (Kwon and Riser, 2004). The seasonal cycle, defined by averaging over each month after subtracting the smoothed time series, is shown for each basin in Fig. 9B. The basic shape of the seasonal cycles in the two basins are similar to each other, and are also consistent both in shape and magnitude with previous research (Davis et al., 2011; Forget et al., 2011). In both basins, the volume peaks late winter and reaches its minimum in late autumn. The peak in late winter is broader in the Atlantic, spanning February through April. Although it looks like a double peak, the error bars indicate that statistically, all three months are within one standard deviation of each other. The Pacific has a

sharper peak in late winter than the Atlantic does, followed by a nearly linear decrease, while the Atlantic has more variability, as indicated by the error bars. Overall, though, the general picture of STMW forming in the late winter and then eroding throughout the year holds in both basins.

6.2. Thickness

The volume of STMW is closely related to the thickness of the thermostad. Fig. 10 shows time series of the average depths of both the tops and bottoms of the STMW layer, as well as the time series of average thickness. The increase in EDW volume in the Atlantic, noted above, is evident in both the increasing thickness of the layer and the increasing depth of the bottom of the layer, while the top is relatively consistent in time. With the trend removed, there is a correlation of 0.70 between the depth of the bottom of the layer and the thickness, and an anticorrelation of −0.72 between the depth of the top of the layer and the layer thickness, indicating that shorter-term variations in thickness result from changes at the top and the bottom of the EDW, while the trend affects only the bottom. There is no statistical correlation between the depths of the top and the bottom of EDW, with or without the trend. In the Pacific, there is a correlation between the thickness of the NPSTMW and the depth of the top of the layer ($r=-0.77$), but the correlation with the depth of the bottom of the layer is much lower at only 0.35. Thus, in the Pacific, thickness is usually controlled by changes in the top of the layer, while the bottom of the mode water layer is unaffected.

Fig. 11 shows maps of the average thickness in each basin. Averages are calculated over the full time series (years 20–119), excluding locations where STMW exists less than 25% of the time.

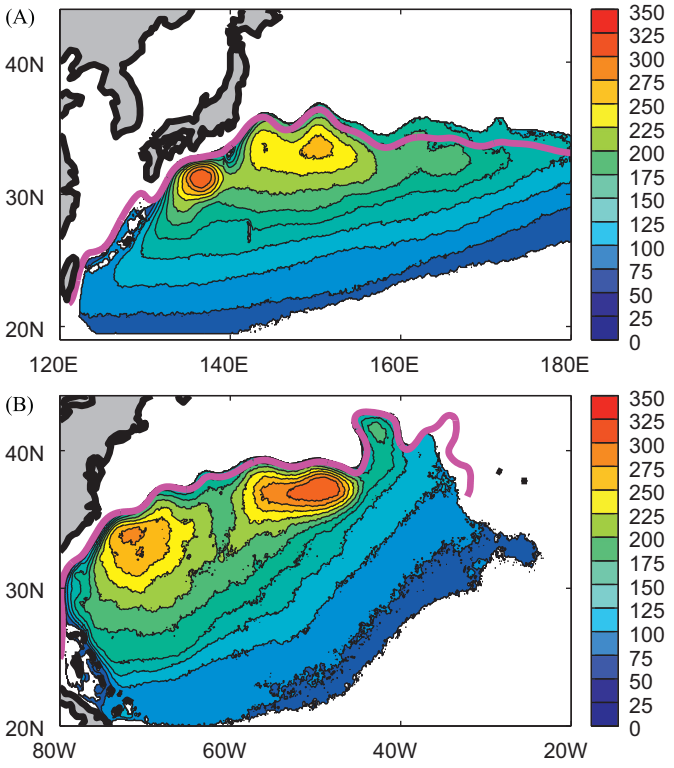

Fig. 11. Average thickness of STMW in each of the two regions. Thick magenta lines show mean locations of the Kuroshio in the Pacific, and the Gulf Stream in the Atlantic (see text for definition). Only locations where STMW existed 25% of the time are shown. (A). Mean thickness of NPSTMW (m) and (B). Mean thickness of EDW (m). (For interpretation of the references to color in this figure legend, the reader is referred to the web version of this article.)

For reference, the axes of the western boundary currents (the Kuroshio in the Pacific, and the Gulf Stream in the Atlantic) are shown. Each of these is defined by an average contour of SSH, 75 cm for the Kuroshio and 0 cm for the Gulf Stream. STMW in both basins forms to the south and east of the western boundary currents. The patterns in the two basins look similar, with one peak close to the separation point and one south of the boundary current jet farther to the east. In the Atlantic, the thickest part of the EDW is in the east, south of the Gulf Stream, as opposed to the Pacific, where the thickest NPSTMW is near the separation point of the Kuroshio. The region with the highest thickness in the Atlantic, centered on 50°W, 35°N, is larger in extent and deeper than the region with the highest thickness in the Pacific, centered on 138°E, 32°N. These patterns are similar to those noted in the discussion of formation, indication that higher formation in a given location occurs when a thick thermostad is ventilated, leading to a thick layer of STMW.

6.3. Core properties

Although by definition STMW is within a certain temperature range, it is interesting to consider how much variability exists within that range over time. One metric for this is examination of the core characteristics. The core of the STMW is defined as the depth of minimum potential vorticity. This is the depth at which the layer is the least stratified, or the most homegeneous. Fig. 12 shows the core depth, temperature, potential vorticity, and age, in both basins. To construct these time series, the depth of the core is determined at each location, and then temperature, potential vorticity, and age are determined at that depth. These properties are then spatially averaged over all STMW, at each time step. In all of these time series, a 12-month running mean has been applied to remove the seasonal cycle and highlight interannual variability.

First, it is clear that the core temperature is much higher in the Atlantic than the Pacific, with a difference is of roughly 1–1.5 °C. While higher temperatures in the Atlantic are expected, the difference is greater than observations would indicate. This is associated with the high temperature model bias in the Atlantic Ocean. There is also a slight downward trend in the core temperature of the EDW, while the NPSTMW has larger variability but no obvious long-term trend. This trend is associated with the spinup of the Atlantic mentioned previously; as the EDW layer thickens, and the bottom of the layer gets deeper, the core cools. With the trend removed, the standard deviation of core temperature of NPSTMW is 0.11 °C, while the standard deviation of EDW temperature is 0.08 °C. The variability noted in the core temperature of the Pacific is slightly less than observed by Hanawa and Kamada (2001), which could be attributable to the lack of atmospheric variability and the associated stability of the Kuroshio Extension. It is also worth noting that in the Pacific, the core temperature is anticorrelated with the NPSTMW volume ($r=-0.70$). When there is more NPSTMW, the core temperature cools. The overall trend in the Atlantic shows a similar pattern, with a long-term decrease in core temperature associated with a long-term increase in EDW. However, if the trend is removed, the correlation disappears as well, indicating that the effect on temperature from short-term variations in EDW volume is unclear.

The core depth in both basins is shown in Fig. 12B. Although Fig. 11 shows large regions of very thick EDW, the spatially-averaged core depth is slightly shallower than in the Pacific. On average the depths of the cores are within 30 m of each other at all times. The core depth shows a deepening trend in both basins throughout the time series, which is in accord with previous comments about the Atlantic but which is somewhat surprising in the Pacific. As with temperature, there is more

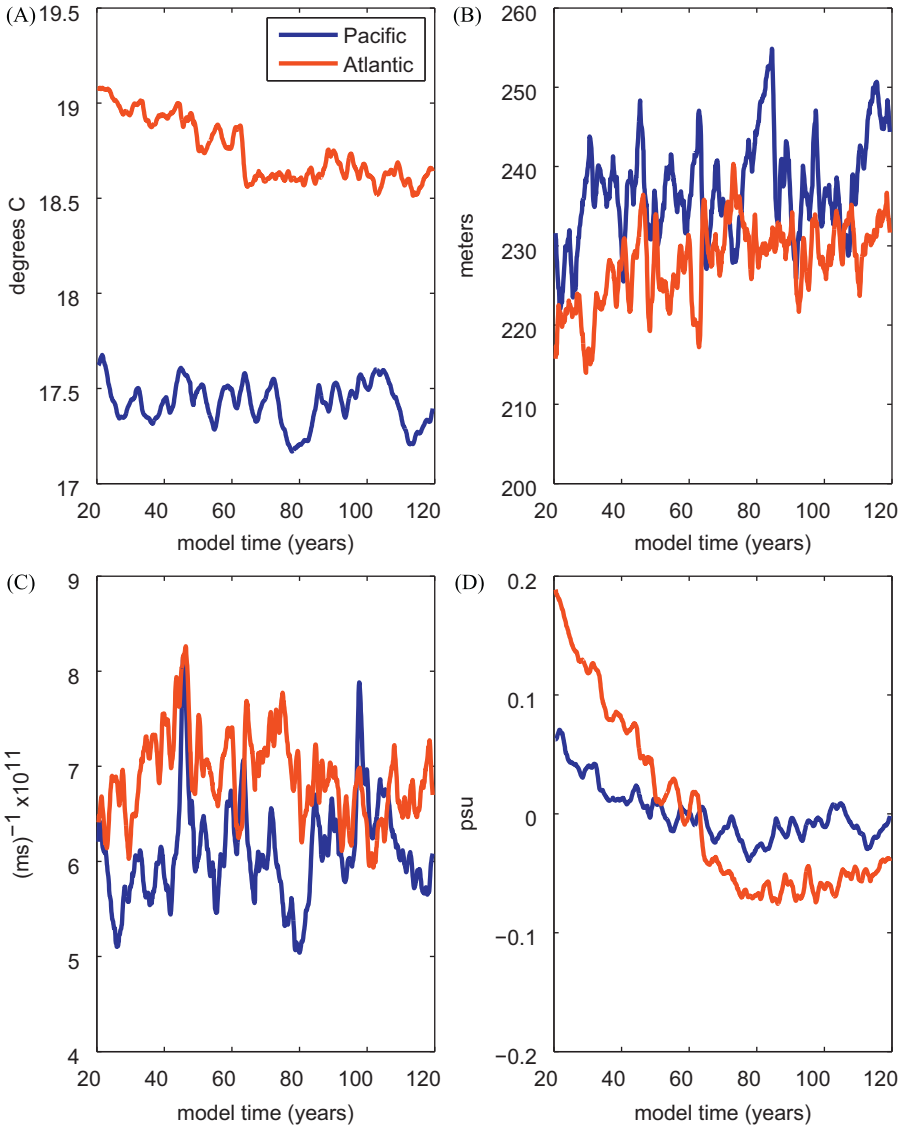

Fig. 12. Core properties of STMW in the two ocean basins. (A) Temperature; (B) Depth; (C) Potential vorticity; (D) Salinity anomaly.

variability in the Pacific, with standard deviation of 5.8 m in a smoothed detrended time series, compared to 3.9 m in the Atlantic. Also similar to temperature, the Pacific has a longer time-scale of variability. On three occasions, the depth increases by around 20 m for 10 or 15 years, and then decreases again. Two of those events are at the same time as the previously noted decreases in core temperature, indicating a broader change in core characteristics. In fact, the detrended time series have a correlation of -0.50. However, there is no correlation between NPSTMW volume and core depth. In the Atlantic, any spikes in depth are smaller (10 m) and shorter-lasting (2 or 3 years). Changes in core depth in the Atlantic are related to changes in total EDW volume, but the relationship is not straightforward. Overall, the core depth and volume of EDW increase throughout the time series, indicating a positive correlation ($r=0.41$). If the trends are removed from both time series, on the other hand, an anticorrelation ($r=-0.43$) can be found. Although both of these values are statistically significant, they are low, and indicate that many factors are influencing the changes in core depth.

Potential vorticity at the core of the STMW also demonstrates some variability. The core PV in the Atlantic varies from about $6–8\times10^{-11}\,\mathrm{m^{-1}\,s^{-1}}$. This is slightly less than the range in observations noted as approximately $5–10\times10^{-11}\,\mathrm{m^{-1}\,s^{-1}}$ (Joyce et al., 2000). However, Joyce et al. (2000) associate that variability with the North Atlantic Oscillation, a large-scale atmospheric signal, so it is not surprising that such variability would not be apparent in the present model output. PV variability has similar time scales in both EDW and NPSTMW, with the EDW demonstrating here longer-term variability similar to that seen in the Pacific. However there are spikes in the Pacific unmatched in the Atlantic, and the standard deviation in the Pacific, at $0.52\times10^{-11}\,\mathrm{m^{-1}\,s^{-1}}$, is slightly greater than that in the Atlantic of $0.44\times10^{-11}\,\mathrm{m^{-1}\,s^{-1}}$. In both basins, volume of STMW is anticorrelated with core PV: the core of a thicker, more homogeneous layer is less stratified than that of a thinner layer. This relationship is stronger in the Pacific (correlation between volume and core PV is -0.87) than in the Atlantic ($r=-0.47$). The relationship is consistent whether or not trends are removed.

On average, EDW is much saltier than NPSTMW. Mean core salinity of EDW is 36.1 psu, while mean core salinity of NPSTMW is 34.7 psu. The modeled value for core salinity in NPSTMW is in line with historical and more recent observations (Masuzawa, 1969; Oka, 2009), while that for the Atlantic is slightly lower than observed (Joyce, 2011; Worthington, 1959). The anomaly of core

salinity in each water mass is plotted in Fig. 12D. It is evident that there is a trend of decreasing salinity in both basins, although it is much more prominent in the Atlantic, especially in the first 50 years or so of the time series. The changes in core salinity compensate the changes in core temperature in both basins, such that the core potential density stays within $\pm 0.1\ \mathrm{kg\,m^{-3}}$ throughout the time series (not shown). After removing a linear trend from each time series, there is still a low anticorrelation ($r=-0.30$) between salinity and STMW volume. This correlation is the same in the Atlantic and the Pacific. A significant difference is that in the Atlantic, the temperature and salinity are very highly correlated. After removal of a linear trend, the correlation is 0.78. In the Pacific, on the other hand, correlation between temperature and salinity is only 0.56, indicating a looser T–S relationship in NPSTMW than in EDW.

Overall, the core properties in the Pacific have stronger correlations with NPSTMW volume than those in the Atlantic have with EDW. Strong correlations exist between NPSTMW volume and core temperature, PV, and potential density and a weak correlation exists between core salinity and volume. In the Atlantic, when the long-term trend is disregarded, correlations between volume of EDW and core depth, PV, salinity and potential density are all relatively weak.

7. Conclusions

This analysis has examined subtropical mode water as it is represented in a model with a climatologically-forced atmosphere. In this simulation, STMW in the Atlantic and Pacific oceans is very similar in both formation and characteristics. There are, however, differences in the details. NPSTMW is thinner, due to shallower mixed layers, evident in the fact that the seasonal deepening of the bottom of the layer is shallower. EDW is more plentiful, and has a longer residence time, even though the percentage that is newly ventilated every year is about the same. This indicates that while EDW in formation regions is ventilated on an annual basis, leading to a high volume of newly renewed EDW, there is also a high volume of EDW that has been subducted and advected away from these ventilation regions. This is confirmed by the long tail of the age distribution of EDW and the higher overall average age, estimated several ways. In the Pacific, younger average ages indicate shorter residence times, and the distribution of ages shows a sharper peak and shorter tail.

This difference in residence time leads to different factors controlling variability in the water masses as well. The volume of newly formed STMW is more highly correlated with total STMW in the Pacific than in the Atlantic, indicating that erosion and its variability is more important in the Atlantic. In the Atlantic, because EDW lasts longer, the memory is longer, and cumulative variability from previous years affects the present volume of EDW. It is likely that this difference in residence time also influences the correlations between core properties that are noted in the Pacific, but are much weaker or nonexistent in the Atlantic. Since southern EDW in particular has not been reventilated, and is preserving the properties from when it was formed, one would not expect the core properties to change due to a large volume of new formation in a given year. In the Pacific, a large volume of new formation will include reventilation of a significant portion of older mode water, and will thus be more likely to reset core properties immediately, resulting in high correlations between changes in volume and changes in core properties. At the same time, the high correlation between core temperature and salinity in EDW shows that although the sizes of the property ranges used for definition of STMW are the same in the two basins, the resulting T–S relationship is tighter in the Atlantic.

Overall, the differences noted here have only been found in a model lacking large-scale long term atmospheric variability. While the interannual variability of various STMW properties in such a regime is interesting, and demonstrates the importance of intrinsic oceanic variability, the next logical step is to understand how these differences and similarities are portrayed in a more realistically-forced model, or, even better, in observations. With the clearer understanding of the intrinsic oceanic variability in each basin, a greater appreciation for the relative impact of large-scale atmospheric variability can be attained.

Acknowledgments

We thank three anonymous reviewers for their very helpful suggestions. E.M.D. acknowledges support of the Doherty Foundation and National Science Foundation (NSF) OCE-0849808. S.R.J was sponsored by the NSF OCE-0849808. Y.-O.K. was supported by the NSF OCE-0961090. The authors thank Frank Bryan and Synte Peacock (National Center for Atmospheric Research) and Mathew Maltrud (Los Alamos National Laboratory) for providing the numerical model output. The simulation was performed at the National Center for Computational Sciences at Oak Ridge National Laboratory with computer time awarded under the INCITE program, and at the National Center for Atmospheric Research Computational and Information Systems Laboratory.

References

Davis, X.J., Rothstein, L.M., Dewar, W.K., Menemenlis, D., 2011. Numerical investigations of seasonal and interannual variability of North Pacific subtropical mode water and its implications for Pacific climate variability. J. Clim. 24, 2648–2665.

Douglass, E.M., Jayne, S.R., Peacock, S., Bryan, F.O., Maltrud, M.E., 2012. Subtropical mode water variability in a climatologically forced model in the Northwestern Pacific Ocean. J. Phys. Oceanogr. 42, 126–140.

Forget, G., Maze, G., Buckley, M., Marshall, J., 2011. Estimated seasonal cycle of North Atlantic Eighteen Degree Water volume. J. Phys. Oceanogr. 41, 269–286.

Hanawa, K., Kamada, J., 2001. Variability of core layer temperature (CLT) of the North Pacific subtropical mode water. Geophys. Res. Lett. 28, 2229–2232.

Hanawa, K., Suga, T., 1995. A review on the subtropical mode water in the North Pacific (NPSTMW). In: Sakai, H., Nozaki, Y. (Eds.), Biogeochemical Process and Ocean Flux in the Western Pacific. Terra Scientific Publishing Company (TERRAPUB), pp. 613–627.

Hanawa, K., Talley, L.D., 2001. Mode waters. Ocean circulation and climate. In: Siedler, J., Church, J. (Eds.), International Geophysics Series. Academic Press, pp. 373–386.

Joyce, T., Deser, C., Spall, M., 2000. The relation between decadal variability of subtropical mode water and the North Atlantic Oscillation. J. Clim. 13, 2550–2569.

Joyce, T.M., 2011. New perspectives on eighteen-degree water formation in the North Atlantic. J. Oceanogr., 1–8.

Joyce, T.M., Thomas, L.N., Bahr, F., 2009. Wintertime observations of Subtropical Mode Water formation within the Gulf Stream. Geophys. Res. Lett. 36, L02607.

Kelly, K.A., Small, R.J., Samelson, R.M., Qiu, B., Joyce, T.M., Kwon, Y.-O., Cronin, M.F., 2010. Western boundary currents and frontal air-sea interaction: Gulf Stream and Kuroshio Extension. J. Clim. 23, 5644–5667.

Kwon, Y., Riser, S., 2004. North Atlantic subtropical mode water: a history of ocean–atmosphere interaction 1961–2000. Geophys. Res. Lett. 31, L19307.

Large, W.G., Yeager, S.G., 2009. The global climatology of an interannually varying air–sea flux data set. Clim. Dynam. 33, 341–364.

Maltrud, M.E., Bryan, F.O., Peacock, S., 2010. Boundary impulse response functions in a century-long eddying global ocean simulation. Environ. Fluid Mech. 10, 275–295.

Masuzawa, J., 1969. Subtropical mode water. Deep-Sea Res. 16, 463–472.

Maze, G., Forget, G., Buckley, M., Marshall, J., Cerovecki, I., 2009. Using transformation and formation maps to study the role of air-sea heat fluxes in North Atlantic Eighteen Degree Water formation. J. Phys. Oceanogr. 39, 1818–1835.

Murray, R., 1996. Explicit generation of orthogonal grids for ocean models. J. Comput. Phys. 126, 251–273.

Oka, E., 2009. Seasonal and interannual variation of North Pacific Subtropical Mode Water in 2003–2006. J. Oceanogr. 65, 151–164.

Qiu, B., Chen, S., 2005. Variability of the Kuroshio Extension jet, recirculation gyre, and mesoscale eddies on decadal time scales. J. Phys. Oceanogr. 35, 2090–2103.

Qiu, B., Chen, S., 2006. Decadal variability in the formation of the North Pacific subtropical mode water: oceanic versus atmospheric control. J. Phys.Oceanogr. 36, 1365–1380.
Qiu, B., Hacker, P., Chen, S., Donohue, K.A., Watts, D.R., Mitsudera, H., Hogg, N.G., Jayne, S.R., 2006. Observations of the subtropical mode water evolution from the Kuroshio Extension System Study. J. Phys. Oceanogr. 36 (3), 457–473.
Rainville, L., Jayne, S.R., McClean, J.L., Maltrud, M.E., 2007. Formation of subtropical mode water in a high-resolution ocean simulation of the Kuroshio Extension region. Ocean Modelling 17, 338–356.
Smith, R., Gent, P., 2002. Reference Manual for the Parallel Ocean Program (POP). Los Alamos Unclassified Report LA-UR-02-2484.
Smith, R., et al., 2010. The Parallel Ocean Program (POP) Reference Manual. Los Alamos Unclassified Report LAUR-10-01853, pp. 1–141.
Suga, T., Aoki, Y., Saito, H., Hanawa, K., 2008. Ventilation of the North Pacific subtropical pycnocline and mode water formation. Prog. Oceanogr. 77, 285–297.
Suga, T., Hanawa, K., 1995. Interannual variations of North Pacific subtropical mode water in the 137-degrees-E section. J. Phys. Oceanogr. 25, 1012–1017.
Suga, T., Hanawa, K., Toba, Y., 1989. Subtropical mode water in the 137-degrees-E section. J. Phys. Oceanogr. 19, 1605–1618.
Talley, L.D., 1996. North Atlantic circulation and variability, reviewed for the CNLS conference. Physica D 98, 625–646.
Talley, L.D., Raymer, M.E., 1982. Eighteen degree water variability. J. Mar. Res. 40, 757–775.
Warren, B., 1972. Insensitivity of subtropical mode water characteristics to meteorological fluctuations. Deep-Sea Res. 19, 1–19.
Worthington, L., 1959. The 18-degree water in the Sargasso Sea. Deep-Sea Res. 5, 297–305.
Worthington, L., 1972. Negative oceanic heat flux as a cause of water-mass formation. J. Phys. Oceanogr. 2, 205–211.